JOURNAL OF CATALYSIS 72, 21–30 (1981)

Strong Oxide–Oxide Interactions in Silica-Supported Fe_3O_4.

III. Water-Induced Migration of Silica on Geometrically Designed Catalysts

CARL R. F. LUND AND J. A. DUMESIC[1]

Department of Chemical Engineering, University of Wisconsin, Madison, Wisconsin 53706

Received April 6, 1981; revised July 14, 1981

Geometrically designed catalysts were prepared by evaporating silica onto part of the surface of an oxidized iron foil. These model catalysts allowed scanning Auger electron microscopy to be used to study the mobility of silica in different gas environments at ca. 670 K and atmospheric pressure. For the iron oxide/silica model catalyst, silica migration was observed upon treatment in H_2O/CO or H_2O/H_2 gas mixtures, while significant migration was not observed upon treatment in CO_2/CO or O_2. In particular, that portion of the iron oxide surface, initially free of Si, became covered by Si after treatment in H_2O/CO or H_2O/H_2, while it remained essentially free of Si after treatment in CO_2/CO or O_2. Preliminary investigation of a similarly prepared Pt/SiO_2 catalyst indicated that the phenomenon of SiO_2 mobility at ca. 660 K and atmospheric pressure may be of importance for other silica-supported catalyst systems.

INTRODUCTION

The first two parts of this series (*1*, *2*) demonstrated that when Fe_3O_4 is supported on SiO_2, a strong oxide–oxide interaction is initiated upon catalyst treatment in a water-containing atmosphere at ca. 660 K. Specifically, this interaction was shown to result from the substitution of Si^{4+} for Fe^{3+} at the tetrahedrally coordinated cation sites of Fe_3O_4, as given by the reaction

$$2SiO_2 + 2[Fe^{3+}](Fe^{2+}, Fe^{3+})O_4 \rightarrow [Si_2{}^{4+}, \square](Fe_2{}^{2+}, Fe_4{}^{3+})O_{12}, \quad (1)$$

where square and round brackets indicate tetrahedral and octahedral sites, respectively. This interaction results in a ferric enrichment of the octahedral sites of Fe_3O_4. Furthermore, it was shown that this reaction forms a Si-substituted shell (ca. 3 atomic layers thick) surrounding a core of nonsubstituted Fe_3O_4. Accordingly, the turnover frequency for the water–gas shift has been found to be several orders of magnitude smaller for silica-supported Fe_3O_4 than for unsupported Fe_3O_4 (*3*). The results of these above studies may be understood in terms of H_2O-induced transport of SiO_2 around the exterior surface of the Fe_3O_4 crystallites followed by substitution according to reaction (*1*). Indeed, chemical transport of SiO_2 by high-pressure steam at high temperatures (e.g., 1.5 MPa steam at 500 K) is well documented (*4–9*); however, this phenomenon has not been observed at ambient pressure, and has been consequently ignored in studies of silica-supported catalysts. This paper and a separate note (*10*) demonstrate the motion of SiO_2 in the presence of H_2O at subatmospheric pressure and ca. 660 K, by direct observation using scanning Auger electron microscopy (SAM; discussed in the present paper) and controlled-atmosphere electron microscopy (CAEM; discussed in Ref. (*10*)). In particular, for the present study, "geometrically designed catalysts" were fabricated by depositing SiO_2 on one-half of an iron oxide surface, and the migration of SiO_2 across the other half of the surface was monitored by SAM. A similar geometrically designed catalyst, fabricated from a

---

[1] Camille and Henry Dreyfus Foundation Teacher-Scholar; to whom correspondence should be addressed.

0021-9517/81/110021-10$02.00/0

Pt foil, was examined using an optical microscope and indicates that SiO_2 mobility may be important in other catalyst systems.

EXPERIMENTAL

A single high-purity (99.99+%) iron foil 0.025 mm (0.001 in.) thick was used to prepare all iron/silica model catalysts. The foil was cleaned by successive rinses in trichloroethylene, toluene, and acetone. All subsequent thermal treatments were effected using the Pyrex gas-handling and kinetics apparatus described elsewhere (*2*); a special Pyrex flow cell was used in place of the chemical reactor. This flow cell featured a suspended basket, fabricated from aluminum screen, in which the foil was contained. All CO/CO_2 gas mixtures were obtained from Matheson (C.P. grade) and passed through a Pyrex tube at 425 K to decompose any trace iron carbonyl present. Oxygen was obtained from Chemetron and used as received. Hydrogen from Chemetron was further purified by passage through an Engelhard "Deoxo" unit followed by activated 13× molecular sieves. Water was twice distilled before use.

The rinsed foil was oxidized in O_2 for 3600 s (1 h) at 670 K and 0.1 MPa. The oxidized foil was then placed on a glass optical microscope slide, and a second slide was placed over one half of the foil, thereby masking one half of the iron oxide surface. After this masked foil was mounted in a vacuum evaporation apparatus (operating at ca. 10^{-3} Pa), an overlayer of SiO_x was deposited onto one half of the iron oxide surface by resistively heating a tungsten dimple-boat filled with a 50:50 mixture of Si and SiO_2. Knowing the distance between the iron foil and the tungsten boat (ca. 0.02 m) and the quantity of Si/SiO_2 in the boat (ca. 0.015 g), the SiO_x overlayer is estimated to be approximately 25 nm thick. After removing the sample from the evaporator a line was scratched on the surface of the foil as close as possible to the interface between the SiO_x-covered and the masked half of the sample. The foil was further oxidized in O_2 at 670 K and 0.1 MPa for 5400 s (1.5 h) and was subsequently cut into several pieces to form four samples, Fe-A through Fe-D, each half-covered by the SiO_x overlayer.

Sample Fe-A received no further thermal treatment. Sample Fe-B was reduced in a 85% CO_2, 15% CO gas mixture at 660 K and 0.1 MPa for 1.8×10^4 s (5 h). Under these conditions, Fe_3O_4 is the thermodynamically stable phase of iron oxide (*11*). Sample Fe-C was reduced concurrently with sample Fe-B and was subsequently placed under the standard water–gas shift conditions of this investigation (*2*, *3*) for 2.9×10^4 s (8 h): 50% H_2O, 45% CO and 5% CO_2 at 663 K and 0.1 MPa. Sample Fe-D was also treated under conditions which thermodynamically produce Fe_3O_4; however, H_2/H_2O was used in place of CO/CO_2. Specifically, the sample treated at 663 K and 0.1 MPa in ca. 50% H_2, 50% H_2O for 9.2×10^4 s (25.5 h). Treatment conditions for samples Fe-A through Fe-D correspond to the conditions used throughout this investigation of silica-supported magnetite (*1*–*3*). Two additional samples, Fe-A′ and Fe-C′, were prepared and treated identically to samples Fe-A and Fe-C with the single exception that they were oxidized in air at 1273 K (instead of at 670 K) after the deposition of the SiO_x overlayer.

Using a Pt foil 2.54×10^{-5} m (0.001 in.) thick, a Pt/SiO_x geometrically designed catalyst was prepared in a manner similar to the Fe_3O_4/SiO_x sample. The only differences in preparation were that the Pt foil was not oxidized prior to evaporation of SiO_x, the Pt/SiO_x interface was not scratched following evaporation, and twice as much Si/SiO_2 was employed (i.e., the SiO_x layer may be estimated as 50 nm thick). The subsequent oxidation of this sample was for 1.8×10^4 s (5 h) at 673 K and 0.1 MPa in O_2. This Pt foil was cut into several pieces. One piece, denoted Pt-A, was exposed to H_2 for 1.8×10^4 s (5 h) at 673 K and 0.1 MPa. A second piece was exposed to ca. 50% H_2, 50% H_2O at 0.1 MPa and 673 K for 1.8×10^4 s (5 h), and labeled as sample Pt-B.

Each iron/silica sample was examined using a Physical Electronics scanning Auger electron microscope at the Exxon Corporate Research Science Laboratories in Linden, New Jersey. (Specimens were stored in sealed mylar envelopes during transit from the University of Wisconsin to Exxon.) Two types of analyses were employed.

Spatial maps of the concentration profiles of Fe and Si on the Fe_3O_4/SiO_x samples were generated with the field of view containing equal areas of the masked and unmasked portions of the sample. The electron beam (ca. 2×10^{-4} m in diameter) was then positioned approximately 1 mm away from the interface and an Auger electron spectrum was collected. These "spot analyses" were performed on both sides of the interface. The Pt/SiO_x samples were examined with an optical microscope.

RESULTS

When the glass microscope slide masks were removed from the iron oxide sample after evaporation, the edge of the SiO_x overlayer was easily visible to the unaided eye. Furthermore the various thermal treatments did not change the visual appearance of the samples.

Figure 1 shows the Fe and Si spatial maps (at magnification of 100×) obtained from sample Fe-A. Figure 2 shows the spatial maps of sample Fe-C. The brightness in these Fe and Si spatial maps is proportional to the peak-to-peak intensity of the Fe Auger electrons at 703 eV and the Si Auger electrons at 76 eV, respectively. The scratch made during preparation is clearly evident in these figures. Figures 3 and 4 show the "spot analyses" of all four Fe samples. Specifically, Fig. 3 shows the Auger electron spectra taken from the unmasked half (i.e., initially SiO_x-covered) of each sample, whereas Fig. 4 shows the spectra of the masked half (i.e., initially Si-free) of each sample. In addition, Figs. 3 and 4 show the "spot analyses" of the sample Fe-D after Ar sputtering for 60 s (5 kV, 25 mA).

As with the iron samples, the Pt/SiO_x interface was clearly visible to the eye after the evaporation masks were removed. In particular, the SiO_x-covered portion of the sample appeared gold in color, while the masked portion had the normal appearance of metallic platinum. Oxidation in O_2 and reduction in H_2 (Sample Pt-A) had no effect on the visual appearance of the samples. After the H_2/H_2O treatment, however, the interface was no longer observable to the unaided eye. Instead, only a few gold-colored "patches" of SiO_x remained on the unmasked side of the Pt foil. This is evident from the photographs of Fig. 5 which show the appearance of samples Pt-A and Pt-B through an optical microscope (at magnifications of ca. 5×). While the original interface was not observable for sample Pt-C in Fig. 5b, it could still be detected by scanning electron microscopy.

DISCUSSION

The effectiveness of the model catalyst preparation technique is demonstrated by Fig. 1. The interface between the iron oxide half of the sample and the iron oxide/silica half of the sample is sharp, at the magnification used in the present study (ca. 100×). Furthermore, a comparison of Fig. 1 with Fig. 2 clearly verifies the previous postulate that silica is mobile under atmospheric-pressure water–gas shift reaction conditions (*2*). Indeed, the Si spatial map shows that the entire surface contains Si after this treatment. Figure 2 also shows that the iron signal from the originally SiO_x-covered half of the sample is essentially absent, while a strong iron signal is emitted from the originally Si-free half. Thus, more SiO_x is on the former half of the sample. It should be noted that the absolute intensity of the Si-signal in Fig. 2b *apparently* indicates that the originally Si-free half of the sample contains more Si than the originally

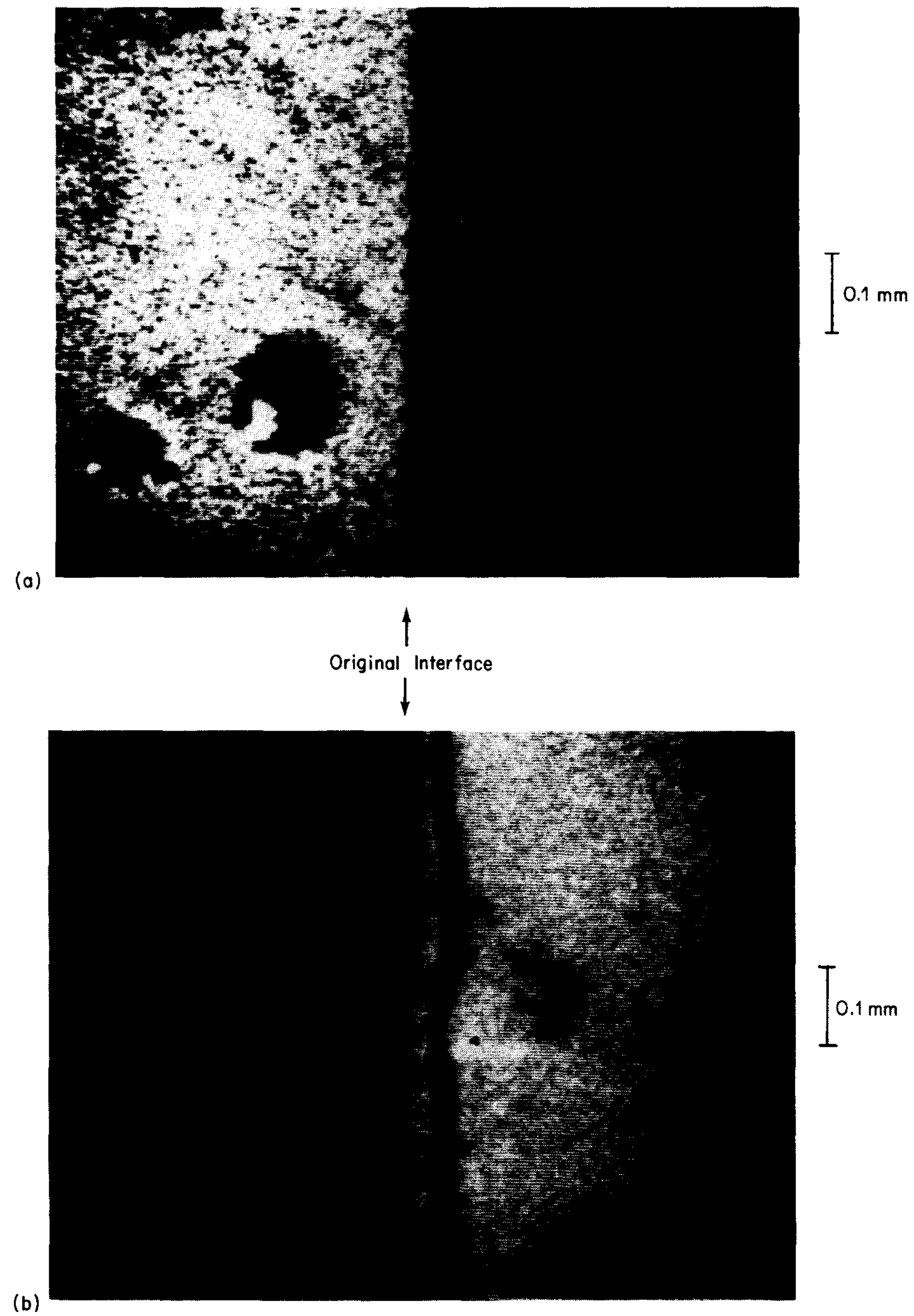

FIG. 1. Scanning Auger electron microscopy spatial maps of sample Fe–A at 100× magnification. Brightness in the maps is proportional to the peak-to-peak intensity of (a) the Fe Auger electrons at 703 eV and (b) Si Auger electrons at 76 eV. The left side of the sample was masked during SiO_x evaporation.

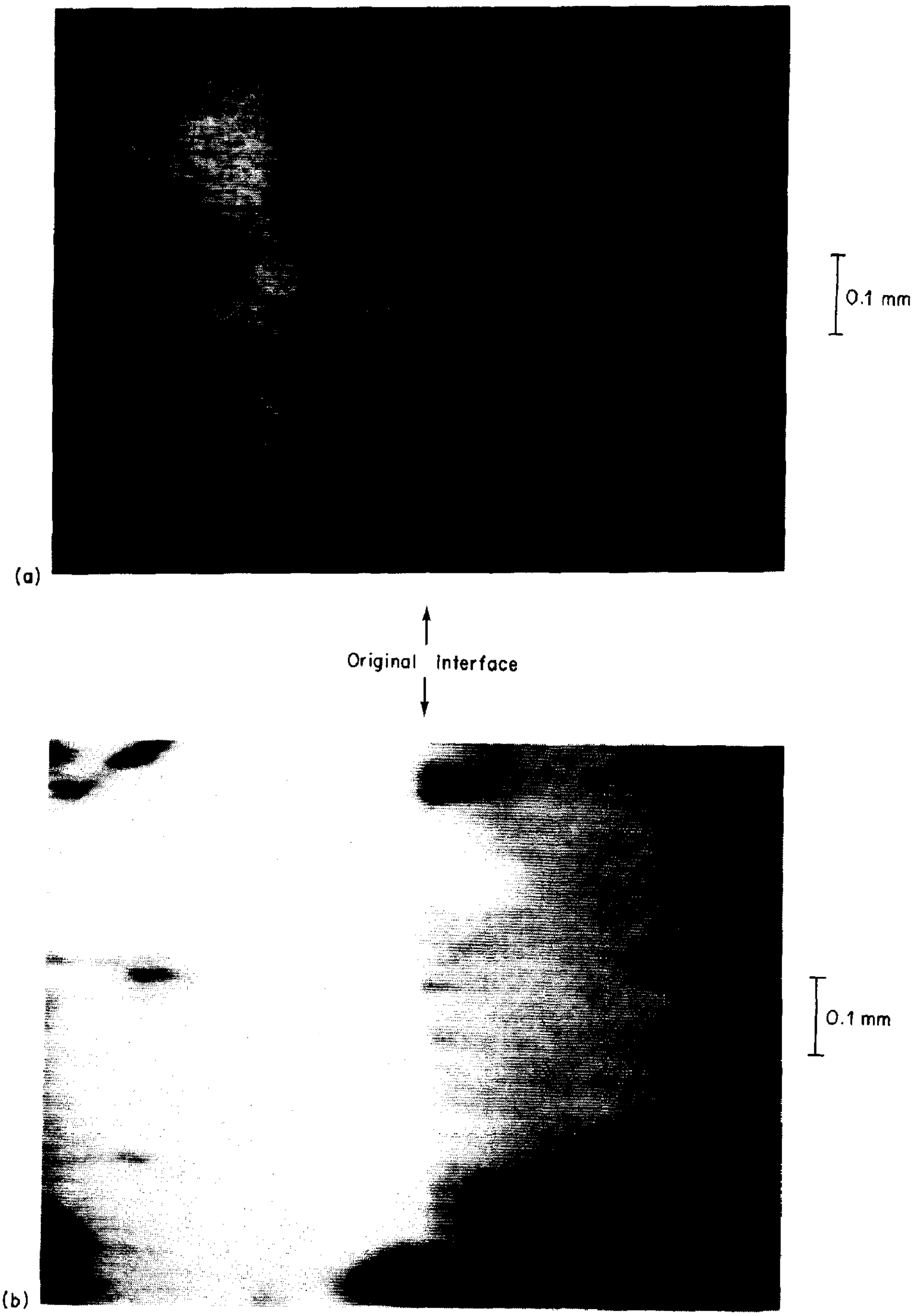

FIG. 2. Scanning Auger electron microscopy spatial maps of sample Fe-C at 100× magnification. Brightness in the maps is proportional to the peak-to-peak intensity of (a) the Fe Auger electrons at 703 eV and (b) Si Auger electrons at 76 eV. The left side of the sample was masked during SiO_x evaporation.

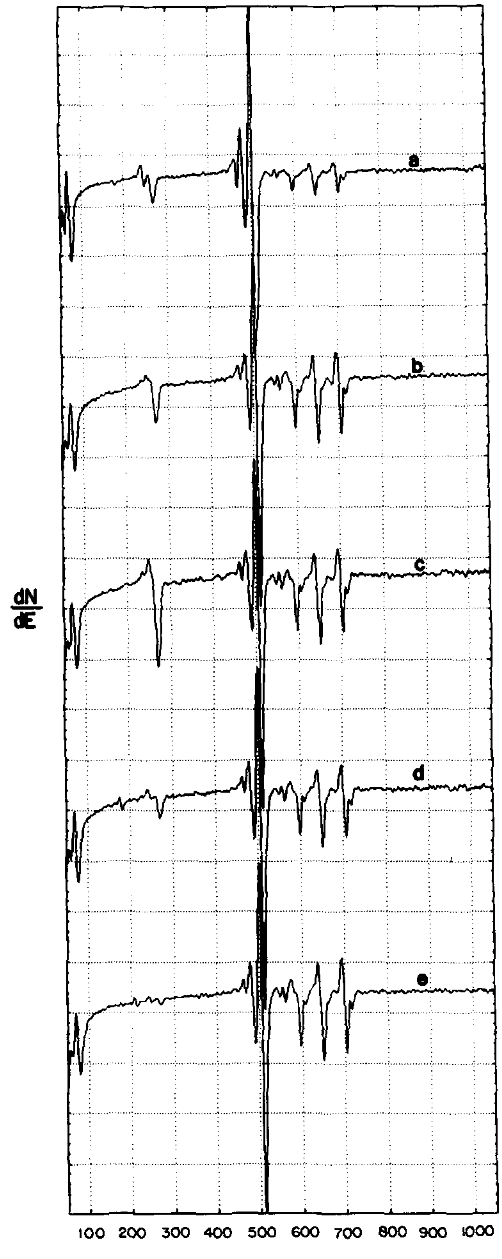

FIG. 3. Auger electron spectroscopy analyses on the unmasked halves (i.e., on SiO_x overlayers) of Fe/SiO_x samples. Analyses were carried out 1 mm away from the edge of the SiO_x overlayer (toward the right as viewed in Figs. 1 and 2). Spectra are normalized by the oxygen peak at 503 eV: (a) Fe-A, (b) Fe-B, (c) Fe-C, (d) Fe-D, and (e) Fe-D after 60 s Ar sputtering.

SiO_x-covered half. This is believed to be an artifact due to differences in the total Auger electron signals from the two halves of the sample. This may result from effects of surface roughness or electron emission from atoms beneath the surface (*12*).

Table 1 presents the ratios of the Fe (703 eV) to Si (76 eV) peak-to-peak intensities measured from the "spot analyses" (see Fig. 4) of the originally Si-free portions of the samples. Clearly, those samples treated in H_2O-containing atmospheres (i.e., Fe-C and Fe-D) show dramatic decreases in the Fe/Si spectral ratio, again evidencing silica mobility in H_2O environments. In fact, the observed (although smaller) decrease in Fe/Si spectral ratio for sample Fe-B (compared to samples Fe-C and Fe-D) may be due to the presence of H_2O in the CO_2/CO gas mixture, since this gas was not dried before use. Additional information about the relative amounts of SiO_x on the two halves of the samples is given by the effects of Ar sputtering, shown in Figs. 3 and 4 for sample Fe-D. In particular, the Si-signal is more greatly diminished (by Ar sputtering) on the originally Si-free half of the sample, compared to the originally SiO_x-covered half. This is consistent with the earlier conclusion that more SiO_x is on the latter half of the sample.

While the present studies of Fe_3O_4/SiO_x model catalyst systems have direct implications in water–gas shift catalysis (*1–3*), the results of Fig. 5 suggest that water-induced migration of silica may be of importance in other catalyst systems as well. Visual com-

TABLE 1

Ratio of Fe(703 eV) to Si(76 eV) Peak-to-Peak Intensities from Masked Halves (i.e., Originally Si-free) of Fe Samples

Sample	Fe/Si ratio
Fe-A	22.8
Fe-B	6.0
Fe-C	1.27
Fe-D	2.0
Fe-D plus 60 s Ar sputter	6.25

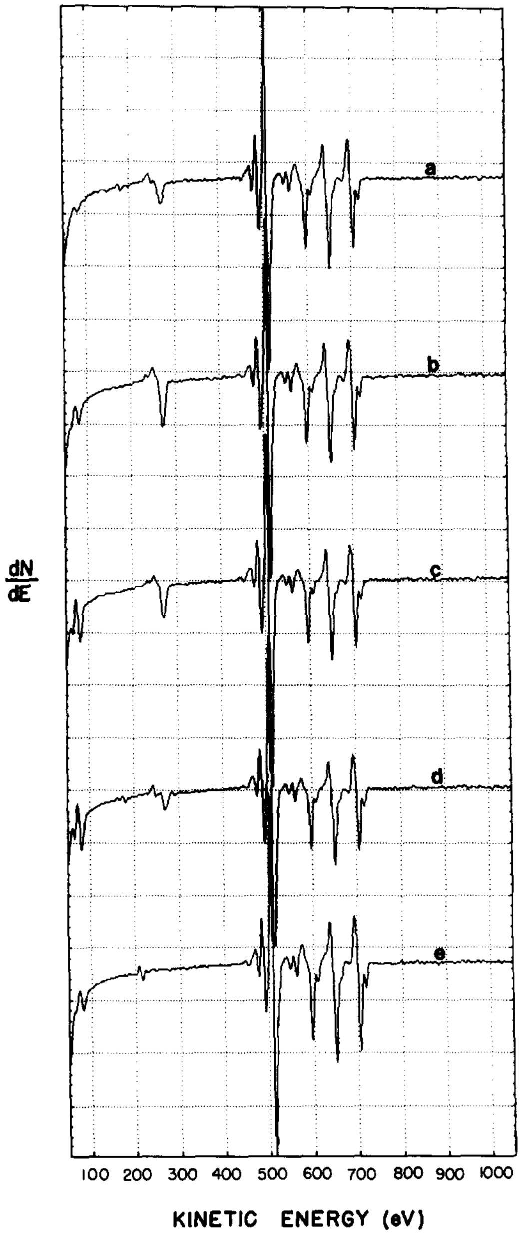

FIG. 4. Auger electron spectroscopy analyses on the masked halves (i.e., originally free of Si) of Fe/SiO_x samples. Analyses were carried out 1 mm away from the edge of the SiO_x overlayer (toward the left as viewed in Figs. 1 and 2). Spectra are normalized by the oxygen peak at 503 eV: (a) Fe-A, (b) Fe-B, (c) Fe-C, (d) Fe-D, and (e) Fe-D after 60 s Ar sputtering.

parison of samples Pt-A and Pt-B through an optical microscope (see Fig. 5) shows that the initially gold-colored SiO_x overlayer (right-hand side of figure) is destroyed by treatment in H_2O/H_2, leaving instead a small number of gold-colored patches. It is apparent that the sample has lost a significant amount of silica.

The vapor-phase transport of silica by steam is well documented (*8*, *9*). It is known to occur at temperatures as low as 472 K (*5*) but has always been observed at elevated pressure (*6*, *7*). Indeed, in the oxidation of Si by steam between 775 and 1225 K, pressure must be carefully controlled or the product SiO_2 is transported away with the steam (*6*). Brady has determined that $Si(OH)_4$ is the most probable vapor-phase-transporting species above 3×10^7 Pa (300 atm), whereas $Si_2O(OH)_6$ is the most likely below this pressure (*7*). Prior to this investigation transport at H_2O pressures less than atmospheric has not been directly observed.

Finally it seems appropriate to briefly comment about the stoichiometries of the silica overlayers, SiO_x, on Fe_3O_4 and Pt. From the literature (*13–16*), it can be estimated that the postevaporation oxidation in O_2 at 670 K would oxidize a single crystal of Si to a depth of 1–3 nm. In the present case, however, the average oxygen content of the silica overlayer after this oxygen treatment is undoubtedly greater than that predicted from Si single-crystal studies. This is because the overlayers are partially oxidized at the outset (i.e., prepared from Si/SiO_2 mixtures) and the overlayers are not highly crystalline. In addition, the subsequent sample treatments (in CO_2/CO, H_2O/CO, H_2O/H_2) will further oxidize remaining Si to SiO_2. Indeed, it can be seen in all of the Auger electron spectra presented that the silicon near the surface of the SiO_x overlayers is present as Si^{4+}. This is true even after 60 s of Ar sputtering (see Fig. 3e). Thus, while the stoichiometry of the SiO_x overlayers remains unknown, it is believed that the value of x is close to 2. Also, since the SiO_x overlayer on Pt is thicker than that on Fe_3O_4, the average value of x in the overlayer may be smaller for the former

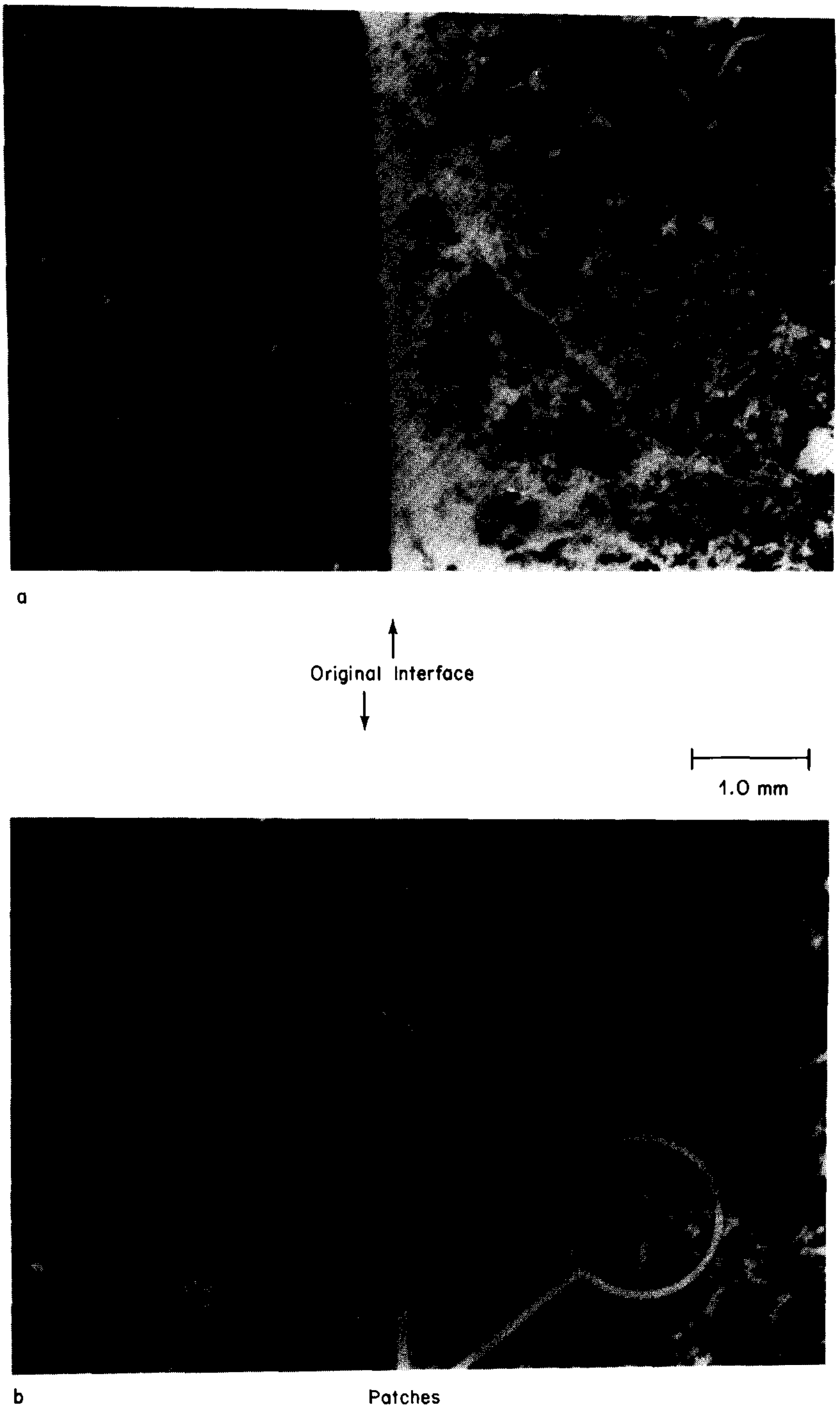

FIG. 5. Optical microscopy photos of Pt/SiO$_x$ samples taken at 5× magnification: (a) Pt-A, (b) Pt-B. The location of edge of the original SiO$_x$ overlayer is indicated and for sample Pt-B two of the SiO$_x$ "patches" are shown.

sample. Most importantly, though, studies of samples Fe-A′ and Fe-C′ (which were oxidized at conditions which would yield $x = 2$) indicate that the value of x does not qualitatively affect the conclusion that silica is mobile in H_2O-containing environments. In particular, Auger electron spectra of these samples were completely analogous to those of samples Fe-A and Fe-C, showing significant transport of silica onto the masked half of the sample Fe-C′ under water–gas shift reaction conditions.

CONCLUSIONS

The transport of SiO_2 in low-pressure, H_2O-containing environments, as proposed by Lund and Dumesic (*2*) from studies of water–gas shift over silica-supported Fe_3O_4, has been confirmed by directly measuring the movement of SiO_2 over Fe_3O_4 and Pt foils half-covered by SiO_2. Furthermore, the usefulness of such geometrically designed catalysts has been effectively demonstrated. The general implication of these findings is that a catalytic surface capable of retaining Si may become contaminated during treatment of silica-containing catalysts in H_2O atmospheres. For example, during the preparation of silica-supported metal catalysts, metals are often added to hydroxylated SiO_2 by impregnation with aqueous solutions. This H_2O may lead to SiO_2-migration during subsequent thermal treatments. Also, any reaction using or producing H_2O could cause SiO_2 migration. Once this mobility has been initiated, the catalytic properties of the silica-containing catalyst could be altered, since it is known, for example, that a silicon-containing adlayer poisons Pt when used in reactions such as methane or carbon monoxide oxidation (*17*).

ACKNOWLEDGMENTS

Acknowledgment is made to the donors of the Petroleum Research Fund, administered by the ACS, for partial support of this research. We would like to acknowledge the financial support of the National Science Foundation through Research Grant ENG 7911130. We thank M. Lagally (University of Wisconsin) for the use of his vacuum evaporator, S. Behal (Exxon) who operated the SAM, and F. S. Delk (Monsanto) who willingly shared his knowledge of SiO_2-transport. R. T. K. Baker and Exxon's Corporate Research Science Laboratories graciously allowed us the use of their facilities for which we wish to express our gratitude. Finally, R. D. Sherwood (Exxon) took the optical microscope photographs of the Pt catalysts, and T. Udovic and T. Hayden (University of Wisconsin) performed the final treatments and Auger analyses of samples Fe-A′ and Fe-C′; and, we wish to thank them for their contribution to this work.

Note added in proof. After this work was accepted for publication, similar Pt/SiO_2 samples were prepared with the primary differences being that these samples had a SiO_2 overlayer ca. 5–10 nm thick and that these samples were treated in O_2 at 1270 K prior to treatment in either H_2 or H_2O/H_2 at 670 K. Transport of Si onto the originally Si-free portion of such a geometrically designed sample was observed by SAM after treatment in H_2O/H_2. The SiO_x overlayer, though did not show the dramatic morphological changes shown in Fig. 5. Thus, the H_2O-induced migration of Si in the Pt/SiO_2 samples of the present study may be exaggerated by the thickness of the overlayer and by the fact that x could be less than 2 for these samples; however, the Pt/SiO_2 samples prepared more recently, for which x should more nearly equal 2, still show that a Si-containing adlayer may form over Pt during treatment of Pt/SiO_2 in H_2O-containing atmospheres.

REFERENCES

1. Lund, C. R. F., and Dumesic, J. A., *J. Phys. Chem.*, in press.
2. Lund, C. R. F., and Dumesic, J. A., *J. Phys. Chem.*, in press.
3. Lund, C. R. F., and Dumesic, J. A., in preparation.
4. Schäfer, H., "Chemical Transport Reactions." Academic Press, New York, 1964.
5. Day, D. E., and Gac, F. D., *Bull. Amer. Ceram. Soc.* **56**, 644 (1977).
6. Kooi, E., "The Surface Properties of Oxidized Silicon," N. V. Phillips Gloeilampenfabrieken. Eindhoven, The Netherlands, 1967.
7. Brady, E. L., *J. Phys. Chem.* **57**, 706 (1953).
8. Prigogine, M., and Fripiat, J. J., *Chem. Phys. Lett.* **12**, 107 (1971).
9. Everett, D. H., Haynes, J. M., and McElroy, P. J., *Nature* **226**, 1033 (1970).
10. Lund, C. R. F., Chludzinski, J., Baker, R. T. K., and Dumesic, J. A., in preparation.
11. Søndergaard, K., *in* "An Investigation on the Kinetics of the Conversion of Carbon Monoxide with Water Vapor over Iron Oxide Based Catalysts," 2nd ed., Haldor Topsøe, Vedbæk, 1969.

12. Davis, L. E., MacDonald, N. C., Palmberg, P. W., Riach, G. E., and Weber, R. E. "Handbook of Auger Electron Spectroscopy," 2nd ed., Physical Electronics Industries, Eden Prairie, Minn., 1976.

13. Deal, B. E., and Grove, A. S., *J. Appl. Phys.* **36,** 3770 (1965).

14. Ruzyllo, J., Shiota, I., Miyamoto, N., and Nishizawa, J., *J. Electrochem. Soc.* **123,** 26 (1976).

15. Hopper, M. A., Clarke, R. A., and Young, L., *J. Electrochem. Soc.* **122,** 1216 (1975).

16. Lora-Tamayo, A., Dominquez, E., Lora-Tamayo, E., and Llabres, J., *Appl. Phys.* **17,** 79 (1978).

17. Gentry, S. J., and Jones, A., *J. Appl. Chem. Biotechnol.* **28,** 727 (1978).